

# ON THE ROLE OF SUB-CORE SCALE HETEROGENEITY DURING REPEATED DRAINAGE/IMBIBITION CYCLES IN A SANDSTONE

Ronny Pini

Department of Chemical Engineering, Qatar Carbonates and Carbon Storage Research Centre, Imperial College London, London, UK

*This paper was prepared for presentation at the International Symposium of the Society of Core Analysts held in Snow Mass, Colorado, USA, 21-26 August 2016*

## ABSTRACT

We present results from an experimental investigation on the hysteretic behavior of the capillary pressure curve for the supercritical CO<sub>2</sub>-water system in a Berea sandstone core. Subcore capillary pressure curves for mm-scale subsets of the rock sample were obtained upon application of a previously developed technique that uses a multi-rate drainage test with simultaneous imaging of gas saturation by X-ray CT. A method is presented to extend this technique to determine scanning imbibition curves at the same scale. This is achieved by profitably combining (i) the measured core-scale drainage capillary pressure curve, (ii) a trapping model and (iii) results from a co-injection experiments carried out at constant total volumetric flow rate and at various gas fractional flow levels. The results confirm that subcore-scale capillary heterogeneity is significant in Berea Sandstone, due to characteristic finer-textured strata that are present also in the sample considered in this study. Previous observations have highlighted the importance of these features to control fluid displacement during drainage; it is shown in this study that the same is true for the re-wetting process. A Brooks-Corey model was successfully applied to describe both drainage and imbibition capillary pressure curves; notably, the latter uses a non-hysteretic formulation, together with the definition of an effective saturation that accounts for the actual amount of mobile phase.

## INTRODUCTION

Deep geological formations behave as capillary systems, because the mechanical equilibrium between the fluids that are present in their porous structure is governed not only by hydrostatic and gravity forces, but also by capillary action [1]. Although the magnitude of the capillary pressure in most reservoirs is usually not large, its effects can be considerable. Of particular interest to this study are situations characterised by repeated flow reversals, which lead to cycles of drainage (wetting phase saturation decreases) and imbibition (wetting phase saturation increases) that may cause disconnected and (temporarily) immobile nonwetting (NW) phase to coalesce and flow again. Such scenario applies to water-flooding operations in oil/gas reservoirs, as well as to the migration of a CO<sub>2</sub> plume in deep saline aquifers within a CO<sub>2</sub> injection and storage scenario.

When repeated flow reversals occur, fluid saturations change in a way that does not solely depend on the current drainage or imbibition process, but also on the history of previous drainage and imbibition cycles; this is known as hysteretic behaviour [2]. The latter directly affects characteristic curves describing multiphase flow, namely capillary pressure and relative permeability curves, which use saturation values that include both mobile and non-mobile fractions. Because these functions are critical input parameters for reservoir simulators, the description of their hysteretic behavior (or lack thereof) has direct bearings on important operational parameters, such as recovery factors or storage capacity estimates [3]. One of key points here is whether the observed NW phase trapping/mobilisation behaviour is consistent when a pore space undergoes repeated cycles of drainage and imbibition, that is, a scenario in which secondary drainage occurs without returning to 100% brine saturation between cycles.

Figure 1 shows a set of results from a recent experimental investigation [4] on the hysteretic behaviour of relative permeability curves for the CO<sub>2</sub>/brine/Berea sandstone system. In the study, a sequence of three drainage/imbibition cycles was completed (A, B and C in the figure) such that (i) the maximum CO<sub>2</sub> saturation of each drainage cycle was greater than that of the previous cycle and (ii) the initial condition was not re-established, i.e. a new drainage cycle always began from previous CO<sub>2</sub> residual saturations. As it can be seen from the figure, the experimental data for the NW phase (CO<sub>2</sub>) fall on several imbibition curves (empty symbols) that differ in the saturation at which imbibition started (turning point). Data on the relative permeability to the wetting phase are not shown in the figure as they were found to follow one single bounding primary drainage and imbibition curve. This last observation is not surprising for systems that possess a strong wetting character, such as the water-wet Berea sandstone. These experimental observations confirm that the core-averaged amount of residually trapped CO<sub>2</sub> is indeed a hysteretic function, while suggesting that this amount increases linearly with the maximum CO<sub>2</sub> saturation reached during each cycle (as discussed in [4]). Notably, relative permeability to the NW phase during imbibition could be well described by using the same functional form as the corresponding non-hysteretic formulation, while modifying the definition of the effective saturation to account for the fraction of NW phase that is effectively mobile.

The main goal of the present work is to extend the analysis of the data reported in [4] by investigating the hysteretic behaviour of the capillary pressure curve at the subcore-scale. In particular, (i) a previously developed experimental approach [5] is applied to quantify capillary heterogeneity within the rock sample at a spatial resolution of  $\sim 10 \text{ mm}^3$  non-invasively and (ii) an extension of the method is presented and applied to determine imbibition capillary pressure curves at the same scale.

## **THEORY**

Capillary pressure-saturation relationships for gas/liquid systems can be described by applying the Brooks-Corey formalism [6] to both drainage ( $D$ ) and imbibition ( $I$ ) processes:

$$P_c^D = P_{c,e} S_w^{*-1/\lambda} \quad (1)$$

$$P_c^I = P_{c,t} (S_{m,w}^{*-1/\lambda} - 1) \quad (2)$$

where  $P_c$  is the capillary pressure,  $P_{c,e}$  is the capillary entry pressure,  $P_{c,t}$  is the capillary pressure at the turning point (i.e. when a new imbibition cycle is started) and  $\lambda$  is the pore-size distribution index. Both relationships are given in terms of effective saturations ( $S_w^*$  or  $S_{m,w}^*$ ), whose definition differ depending on whether drainage or imbibition takes place [7]. In particular, during imbibition a distinction has to be made between the amount of non-wetting (NW) phase that is still mobile and the amount that remains trapped (and disconnected) in the pore space. Only the former contributes to flow and, accordingly, should be used to compute relative permeability (and capillary pressure) values. The effective water saturation ( $S_w^*$ ) and the effective *mobile* water saturation ( $S_{m,w}^*$ ) are defined as follows:

$$S_w^* = \frac{S_w - S_{w,irr}}{1 - S_{w,irr}} \quad (3)$$

$$S_{w,m}^* = 1 - S_{nw,m}^* = 1 - \left( S_{nw}^* - \left[ S_{nw,r}^* (S_{nw,turn}^*) - S_{nw,r}^* (S_{nw,m}^*) \right] \right) \quad (4)$$

where  $S_{w,irr}$  is the (constant) irreducible wetting phase saturation, and  $S_{nw}^*$ ,  $S_{nw,m}^*$ ,  $S_{nw,r}^*$  are the total, mobile and residual effective saturation of the NW phase [7]. Residual NW phase saturations refer to the amount trapped at  $P_c = 0$  and are typically described by means of so-called trapping models, which use the saturation at turning points ( $S_{nw,i}$ ) as the sole independent variable, i.e.  $S_{nw,r}^* = f(S_{nw,i})$  [7]. As such, the total NW saturation can be computed as the sum of mobile and (currently) trapped saturations, the latter being term within square brackets in Eq. 4, that is, the difference between the ultimate residual NW phase saturation (at  $P_c = 0$ ) and the amount yet to be trapped.

As an example of general validity, Figure 2 shows bounding and scanning capillary pressure-saturation curves obtained upon application of the model just described. The system considered is the one from the study by [4] that was presented in the Introduction section. The parameter set used for computing the capillary pressure curves is summarized in Table 1. For the calculations, a linear model was used to represent NW phase trapping, i.e.

$$S_{nw,r}^* = C S_{nw,i} \quad (5)$$

where  $C$  is a constant that represents the trapping fraction. This model was found to describe NW phase trapping for the Berea Sandstone core used in [4] in the range  $0 < S_{nw,i} < 0.6$ . As confirmed by the experiments presented in the same study, we have also

assumed in the model calculations that scanning curves during drainage are equal to the corresponding imbibition curves until the primary (bounding) drainage curve is reached.

## METHODS

### Rock Sample, Fluids and Experimental Parameters

A 930mD Berea Sandstone core (length: 10 cm, diameter: 5 cm) was used that has an average porosity of 22% with minimal variations along its length (maximum variation of about  $\pm 0.2\%$ abs. and  $\pm 3\%$ abs. for slice- and voxel-averaged values, respectively, as measured by x-ray CT). Carbon dioxide (CO<sub>2</sub>) and tap water were used as the operating fluids for the core-flooding experiments. Experimental conditions were: temperature of 50°C, pore fluid pressure of 9 MPa and confining pressure of 13 MPa. The viscosity of the fluids are taken to be  $\mu_{\text{CO}_2} = 2.3 \times 10^{-5}$  Pa×s and  $\mu_w = 5.5 \times 10^{-4}$  Pa×s for CO<sub>2</sub> and water, respectively. X-ray CT scans have been acquired with a voxel dimension of (0.5×0.5×1) mm<sup>3</sup>, tube current 200 mA, energy level of the radiation 120 keV, display field of view 25 cm. The image that is obtained is further resampled into (2×2×3) mm<sup>3</sup> voxels, thus reducing the uncertainty associated with the computed saturation values at the voxel scale to 4.5%abs. [5]. Note that this voxel volume contains approximately 4500 grains and it is well above the minimum REV typically considered for sandstones; this further implies that it can be associated to continuum-scale properties, such as porosity, permeability, fluid saturation, and capillary pressure.

### Core-flooding Experiment

The detailed experimental procedure together with a description of the experimental set-up for the core-flooding experiment is given elsewhere [4]. Briefly, three cycles of drainage and imbibition were completed to collect steady-state saturation and relative permeability data (shown in Figure 1 and referred to as A, B, and C in chronological order). The experiment started with the rock sample fully saturated with water, followed by the co-injection of the pre-equilibrated fluids at different fractional flows ( $f_g$ ) and at a total flow rate of 21 ml/min. The fractional flow of CO<sub>2</sub> was increased or decreased between steps, depending on whether a drainage or imbibition loop was to be completed. The first and the second cycles (A and B in Figure 1) were interrupted before reaching  $f_g = 1$  (during drainage) and  $f_g = 0$  (during imbibition). The main reason for this was to maintain a relatively flat saturation within the core throughout the experiment, a condition that can indeed be met only during co-injection. Accordingly, the second and third drainage cycles began from previous CO<sub>2</sub> residual saturations and not from re-established initial conditions ( $S_w = 1$ ). After reaching  $f_g = 1$  during the final cycle (C), the total CO<sub>2</sub> flow rate was increased in steps from 21 up to 51 mL/min. Results from this multi-rate flood have been used to estimate the core-scale capillary pressure-saturation curve, by following the method described in [10] and again summarized below. Data reconciliation is carried out using two measured variables, namely the pressure drop across the core and fluid saturations (measured by x-ray CT scanning). A minimum of 10 pore volumes (PV) was allowed to pass through the core at each fractional flow (or flow rate during the multi-rate core-flood) before taking a scan. Pressure readings for subsequent calculations were collected over the duration of the x-ray scan, in which time

approximately 1.8 pore volumes of flow occurred. For each step, standard deviations of pressure drop were within 5% of the average pressure drop.

### **Subcore-scale Drainage and Imbibition Capillary Pressure Curves**

As originally proposed in [8,9] and later adopted in [10] for the scCO<sub>2</sub>/water system, multi-rate core-flood carried out at  $f_g = 1$  can be used to directly estimate a *drainage* capillary pressure curve for the system under study, by combining the pressure drop values measured across the core at steady-state and at each flow rate with the corresponding water saturations observed at the inlet face of the core (by e.g., x-ray CT). Remarkably, the method described can be extended to the measurement of subcore-scale  $P_c(S)$ -curves at any position within the sample non-invasively [5]. Two conditions are required to justify this extension: (i) the fluids are in capillary equilibrium throughout the sample and (ii) the functional relationship between capillary pressure and saturation that is obtained for the inlet slice is valid for any other slice within the sample. As shown in the Results section these two conditions are indeed met for the experiments presented here. Therefore, a capillary pressure profile along the length of the sample can be derived from the known core-scale  $P_c(S)$  functional relationship and measured slice-averaged saturations (by x-ray CT), and subcore-scale *drainage* capillary pressure curves are constructed by linking these capillary pressure values to the saturation observed in each subset (voxel) of a given slice. In this study, subcore-scale *imbibition* capillary pressure curves have been constructed in a similar manner, although during co-injection (rather than single-phase injection), so as to maintain a flat saturation profile within the core sample. In particular, once steady state is reached at a given fractional flow, the mobile core-average NW phase saturation is computed from Eq.4 and the corresponding core-average capillary pressure is obtained from Eq.2. Subcore-scale *imbibition* capillary pressure curves are then constructed by linking these capillary pressure values to the saturation observed in each subset (voxel).

## **RESULTS**

### **Multi-rate Drainage Core Flood**

Figure 3 shows the steady-state 1-D slice-averaged CO<sub>2</sub> saturation profiles along the length of the core that were acquired at three different flow rates (21, 31, 51 mL/min) during the multi-rate core-flood carried out at  $f_g = 1$ . In the figure, symbols represent gas saturations estimated from x-ray CT measurements, whereas the solid lines are model predictions. The latter have been obtained from the numerical solution of the steady-state 1-D formulation of Darcy's equation for multiphase flow expressed in differential form. For the calculations, the model assumes a constant slice-average permeability and a Brook-Corey formulation for both the capillary pressure and the NW phase relative permeability curves [11] (parameters given in Table 1). Note that the parameters used in the model were obtained upon fitting the Brooks Corey equation to the core-scale  $P_c-S$  data measured using the experimental protocol described above. The agreement between experiment observations and model predictions is very good, thus enabling the verification of the assumption of capillary equilibrium during displacement, while confirming (i) the homogeneity of Berea Sandstone at the core-scale and (ii) the validity

of the proposed set of parameter values used in the two multiphase characteristic functions to capture displacement at the macroscopic scale.

### Sub-Core Scale Capillary Heterogeneity

The method described above has been extended to the measurement of subcore scale  $P_c(S)$ -curves at any position within the sample [5]. The result of this exercise is presented in Figure 4, where a 3-D reconstruction of the rock sample is shown in terms of so-called capillary pressure scaling factors:

$$\alpha_i = \bar{P}_c(S) / P_{c,i}(S) \quad (6)$$

The latter relate capillary pressure values measured at any given location  $i$  within the sample to a representative mean (i.e. the value representative for a whole slice) [5]. When a Brooks-Corey formulation is used to describe the  $P_c$ - $S$  relationship, these scaling factors represent the ratio between the sample- and the voxel-capillary entry pressure values. As such, these scaling factors can be used to represent and quantify spatial heterogeneity in rock cores. As presented in Figure 4, these scaling factors deviate up to 20% from the mean even for a “homogeneous” rock, such as Berea Sandstone. Notably, (i) the strength of heterogeneity is similar in order to the one observed previously in another sample of the same rock type (but with significantly different average permeability) [5] and (ii) the heterogeneity is present in the form of a stratification that is oriented sub-parallel to the axis of the core; the latter is very likely associated to finer-textured strata that are often observed in Berea Sandstone cores [6].

### Quantitative Imaging of Imbibition at the Sub-Core Scale

As explained above, fluid distribution within the core was observed in real time by x-ray CT throughout the study, thus allowing for precise quantification of fluid saturation at a resolution of about  $(2 \times 2 \times 3) \text{ mm}^3$ . Figure 5 shows 2D  $\text{CO}_2$  saturation maps of a selected slice within the core that have been acquired during imbibition cycle B (with reference to Figure 1) at various fractional flows  $f_g$  after attaining steady-state. To facilitate comparison, the corresponding map of capillary scaling factors is shown in the center of the figure. Generally, the spatial distribution of  $\text{CO}_2$  within each slice is very heterogeneous and, as expected, it correlates with distinct features observed in the capillary scaling map. The presence of a finer-textured stratification is readily visible and its effects are manifested in little NW phase penetrating that region of the sample during drainage. During imbibition, the same stratification is the first to be re-wetted by water, followed by the surrounding portion of the slice.

### Sub-Core Scale Drainage and Imbibition Capillary Pressure Curves

Subcore-scale capillary pressure curves are shown in Figure 6 that belong to two voxels selected within the same slice analysed in Figure 5; these are characterized by an early and a late filling with the NW phase during drainage, respectively. The former has a scaling factor  $\alpha_i > 1$ , while for the latter  $\alpha_i < 1$ , i.e. a *larger* capillary pressure is required

to reach the same saturation as the core-averaged value. In the figure, data acquired during drainage are represented by the empty symbols and include all cycles, while only cycle B is shown for measurements taken during imbibition (filled symbols). It can be seen that these mm-scale capillary pressure curves are distinct from each other, thus confirming the significant degree of heterogeneity at this scale. These measurements validate previous numerical [12] and experimental [5,10] findings on the existence of spatially varying capillary pressure curves, and extend them for the first time to imbibition conditions. In the figure, the solid (drainage) and dashed (imbibition) curves represent predictions based on the Brooks-Corey model (parameters given in Table 1). While for drainage conditions, the capillary scaling factor  $\alpha_i$  has been used as a fitting parameter to match the subcore-scale measurements, in the case of imbibition the curves are used in a truly predictive manner. The agreement between experiment and model is striking and supports the applicability of a scaling relationship at the sub-core scale, as would be expected from the Leverett J-Function relationship [13]. Furthermore, these results suggest that the same trapping model applies at the core- and subcore-scale. More experiments with other rock types with e.g., more pronounced heterogeneities, are needed to assess the general validity of this simple scaling approach and conclusions.

## CONCLUSIONS

In this study, results have been presented from a detailed experimental investigation on the role of subcore-scale heterogeneity during drainage and imbibition processes in Berea sandstone with the supercritical CO<sub>2</sub>-water system. Heterogeneity is quantified by evaluating the capillary pressure-saturation relationship at various scales. An extension of a previously developed method has been presented that now enables such measurements to be carried out during both drainage and imbibition conditions in a core-flood. Capillary pressure curves obtained non-invasively for mm-scale subsets of the rock sample follow a simple scaling relationship and can be well captured by means of the well-known Brooks-Corey relationship. Notably, the latter (i) was applied through a non-hysteretic formulation that uses an effective saturation that accounts for the actual amount of mobile phase and (ii) correctly predicts the imbibition curves by using a linear trapping model. These results emphasize once more the importance of such detailed observations and measurements in the context of core-analyses, because rocks are inherently complex and can rarely be treated as ‘uniformly heterogeneous’.

## ACKNOWLEDGEMENTS

The analysis presented herein was done on a core-flooding experiment that was carried out at Stanford University in collaboration with Prof. Sally Benson. The author gratefully acknowledges funding from the Qatar Carbonates and Carbon Storage Centre (QCCSRC), provided jointly by Qatar Petroleum, Shell and Qatar Science & Technology Park.

## REFERENCES

1. Dullien F. *Porous media. Fluid transport and pore structure*. Academic Press Inc., London, (1992).
2. Craig, F.F. “The Reservoir Engineering Aspects of Waterflooding”, *SPE Monograph Series*, 1971, **3**.
3. Doughty, C., “Modeling geologic storage of carbon dioxide: comparison of non-hysteretic and hysteretic characteristic curves”, *Energy Conversion Management*, 2007, **8**, 1768-81.
4. Ruprecht, C., R. Pini, R. Falta, S. Benson, L. Murdoch, “Hysteretic trapping and relative permeability of CO<sub>2</sub> in sandstone at reservoir conditions”, *International Journal of Greenhouse Gas Control*, 2014, **27**, 15-27.
5. Pini, R. and S. M. Benson, “Characterization and scaling of mesoscale heterogeneities in sandstones”, *Geophysical Research Letters*, 2013, **40**, 1-6.
6. Brooks, R. H., and A. T. Corey, “Hydraulic properties of porous media”, *Hydrology Paper-Colorado State University*, 1964, **3**, 1–27.
7. Land, C. S., “Calculation of imbibition relative permeability for two- and three-phase flow from rock properties”, *SPE Journal*, 1968, **8**, 149-56.
8. Ramakrishnan, T. S. and Cappiello, A., “A new technique to measure static and dynamic properties of a partially saturated medium”, *Chemical Engineering Science*, 1991, **46**, 1157-1163.
9. Lenormand, R. and Eisenzimmer, A., “A novel method for the determination of water/oil capillary pressures of mixed wettability samples”, paper 9322, Society of Core Analysis, Houston, USA, 1993.
10. Pini, R., S. C. M., Krevor, and S. M., Benson, “Capillary pressure and heterogeneity for the CO<sub>2</sub>/water system in sandstone rocks at reservoir conditions”, *Advances in Water Resources*, 2012, **38**, 48–59.
11. Pini, R. and S. M. Benson, “Simultaneous determination of capillary pressure and relative permeability curves from core-flooding experiments with various fluid pairs”, *Water Resources Research*, 2013, **49**, 1-15.
12. Krause, M., J.-C., Perrin, S. M., Benson, “Modeling permeability distributions in a sandstone core for history matching coreflood experiment”, *SPE Journal*, 2011, **16**, 768–77.
13. Leverett, M. C., “Capillary behavior in porous solids”, *Petroleum Transactions (AIME)*, 1941, **142**, 152–69.

Table 1: Brooks-Corey parameters used for the calculations presented in this study

$P_{c,e}$ [kPa]	$S_{w,irr}$ [-]	$\lambda$ [-]	$C$ [-]
2.73	0.301	0.54	0.45



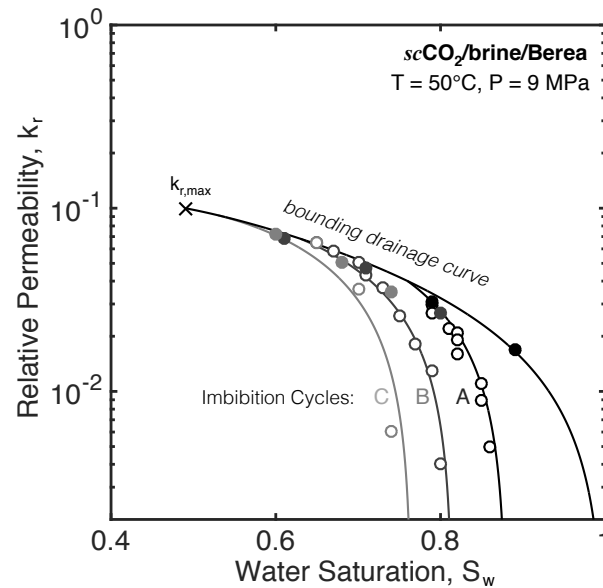


Figure 1. Drainage (full symbols) and imbibition (empty symbols) relative permeability curves of the NW phase ( $\text{CO}_2$ ) as a function of water saturation (wetting phase). The three scanning cycles have been carried out in the sequence A, B, C. Data re-plotted from [4].

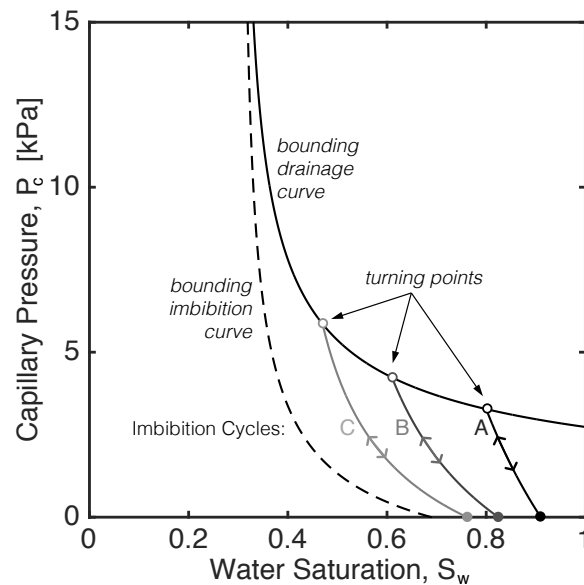


Figure 2. Drainage (solid black line) and imbibition (dashed black line) capillary pressure curves as obtained from the Brooks-Corey relationship, Eqs. 1 and 2, using the parameters listed in Table 1. Three scanning curves (A, B, C) are additionally shown that have been predicted upon application of the method described in the “Theory” section.

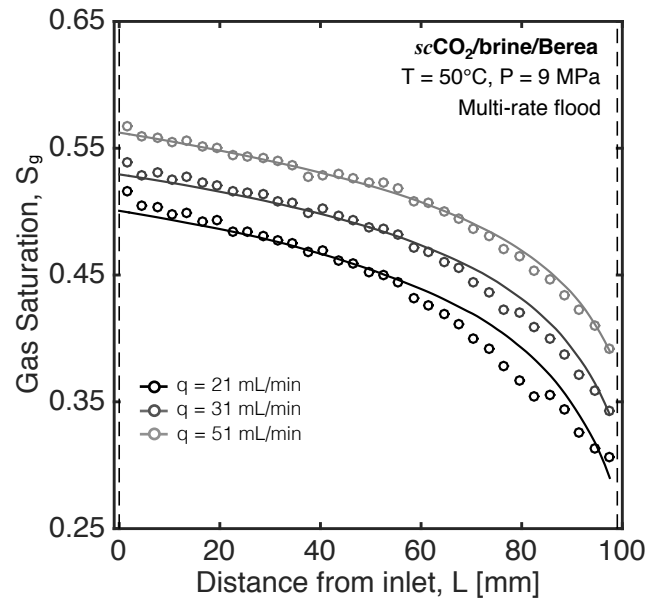


Figure 3. 1D slice-averaged CO<sub>2</sub> saturation profiles along the length of the core sample obtained at three distinct flow rates (21, 31 and 51 mL/min). Symbols represent in-situ measurements by X-ray CT scanning, while solid lines are predictions from the 1D model described in section “Multi-rate Drainage Core Flood”.

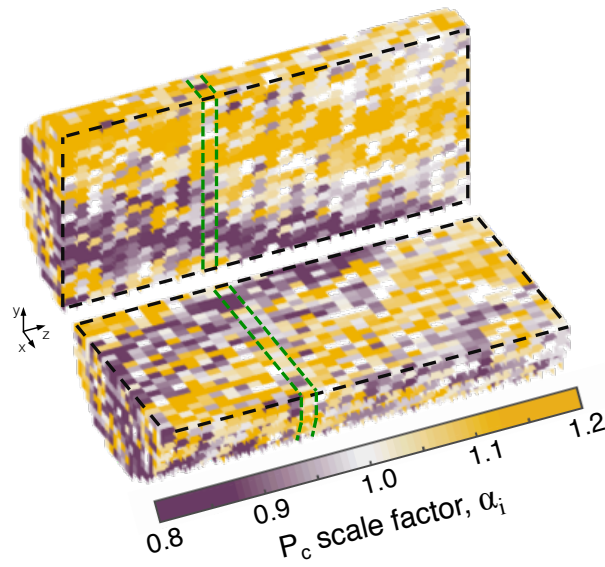


Figure 4. 3D representation of the rock sample used in this study in terms of a capillary scaling factor that reflect sub-core scale capillary heterogeneity. Both vertical and horizontal cross-sections are shown that have been obtained upon virtually slicing the sample along the longitudinal (z) direction. The highlighted vertical slice is the one represented in Figure 5. Voxel size is  $(2 \times 2 \times 3)$  mm<sup>3</sup>.

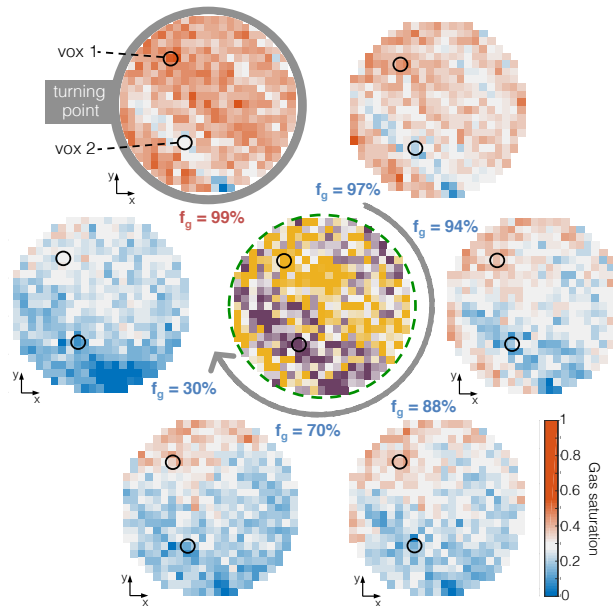


Figure 5. Time evolution of gas saturation in a single slice within the rock sample during an imbibition cycle. The turning point ( $f_g = 99\%$ ) is shown on the top left and imbibition evolves clockwise down to a fractional flow of  $f_g = 30\%$ . The color map represents gas saturation with the exception of the central 2D map where the capillary scaling factor is shown (see also Figure 4). The small circles highlight two specific voxels for which sub-core scale capillary pressure curves have been evaluated, as shown in Figure 6.

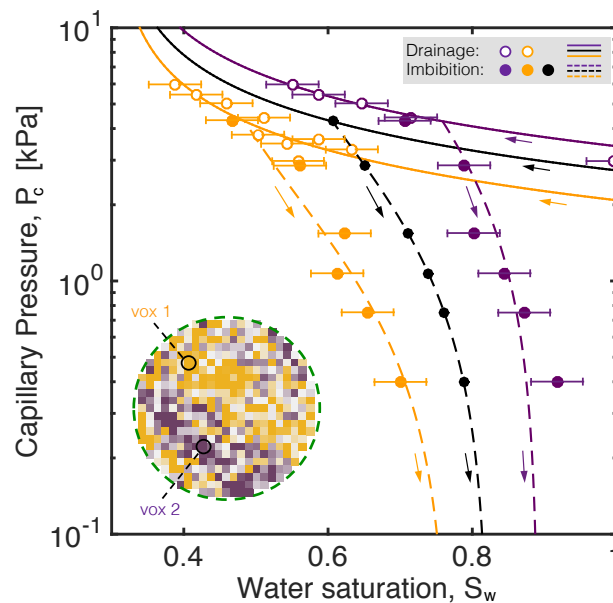


Figure 6. Sub-core scale drainage (solid lines, empty symbols) and imbibition (dashed lines, filled symbols) capillary pressure curves for the  $\text{scCO}_2/\text{water}/\text{Berea Sandstone}$  system. The core-average capillary pressure curves are shown in black, while the coloured curves are representative of two specific voxels within the same slice, as highlighted in the inset. Symbols represent experimental measurements, while solid and dashed lines are model predictions.